J Mol Model (2013) 19:943–949
DOI 10.1007/s00894-012-1634-6

ORIGINAL PAPER

Nitrous oxide adsorption on pristine and Si-doped AlN nanotubes

Javad Beheshtian · Mohammad T. Baei · Ali Ahmadi Peyghan · Zargham Bagheri

Received: 23 August 2012 / Accepted: 7 October 2012 / Published online: 25 October 2012

Abstract Using density functional theory, we studied the adsorption of an N_2O molecule onto pristine and Si-doped AlN nanotubes in terms of energetic, geometric, and electronic properties. The N_2O is weakly adsorbed onto the pristine tube, releasing energies in the range of −1.1 to −5.7 kcal mol^{-1}. The electronic properties of the pristine tube are not influenced by the adsorption process. The N_2O molecule is predicted to strongly interact with the Si-doped tube in such a way that its oxygen atom diffuses into the tube wall, releasing an N_2 molecule. The energy of this reaction is calculated to be about −103.6 kcal mol^{-1}, and the electronic properties of the Si-doped tube are slightly altered.

Keywords Doping · Nanostructures · DFT · Computational study · Nanotube

J. Beheshtian
Department of Chemistry,
Shahid Rajaee Teacher Training University,
P.O. Box: 16875–163, Tehran, Iran

M. T. Baei
Department of Chemistry,
Azadshahr Branch, Islamic Azad University,
Azadshahr, Golestan, Iran

A. A. Peyghan (✉)
Young Researchers Club, Islamic Azad University,
Islamshahr Branch,
Tehran, Iran
e-mail: ahmadi.iau@gmail.com

Z. Bagheri
Physics Group, Science Department, Islamic Azad University,
Islamshahr Branch, Islamshahr, P.O. Box: 33135–369, Tehran,
Iran

Introduction

Until recently, nitrous oxide (N_2O) was regarded as a relatively harmless substance. Although N_2O does not belong to the category of pollutants known as NO_x, it has recently been found to contribute to the destruction of the ozone layer in the stratosphere, and is now a recognized greenhouse gas [1, 2]. N_2O is emitted from natural sources and through human activities, such as the production of adipic acid and nylon. N_2O is thermodynamically unstable, but the homogeneous thermal decomposition reaction does not occur until 625 °C. The decomposition reaction of N_2O over various catalysts, and in particular over inorganic surfaces, has been studied quite intensively because of the environmental problems connected with the release of this molecule into the atmosphere during industrial processes such as the production of fertilizers and polymer fibers, or from car exhausts [3, 4].

Carbon nanotubes (CNTs) were identified for the first time by Iijima in 1991 as by-products of arc discharge experiments [5]. They are light and flexible, have a high elastic modulus, and show electronic properties that are dependent on their diameters and chiralities [6]. These unusual features mean that CNTs are candidates for various applications in nanoengineering [7–9], and they led to the discovery of new physical properties associated with quasi-one-dimensional structures. For instance, tubular structures of group III–V compounds have been theoretically predicted [10] and experimentally synthesized [11], with promising applications being envisioned in many different areas. Zhang et al. predicted that AlN nanotubes (AlNNTs) are energetically favorable and that they take the form of a hexagonal network with sp^2 hybridization for both N and Al atoms [12]. Tondare et al. successfully synthesized

AlNNTs with diameters ranging from 30 to 80 nm [13]. Recently, other papers have reported the synthesis of AlNNTs through different methods [14–16].

Gas adsorption on CNTs and nanotube bundles is an important issue in both pure research and that relating to nanotube applications. The adsorption characteristics of nanotubes in the gas phase have prompted their utilization in gas sensors, fuel storage, and the reduction of hazardous pollutants from gas streams [17–19]. To this end, in the work described in the present paper, we tried to answer the following questions: (1) can AlNNTs provide a suitable surface for N_2O dissociation, and (2) if not, what strategy can be applied to improve the applicability of AlNNTs to N_2O dissociation?

Computational methods

Geometry optimizations, natural bond orbital (NBO), and density of states (DOS) analyses were performed on a (5, 0) zigzag AlNNT (constructed from 30 Al and 30 N atoms) and different N_2O/AlNNT complex configurations at the B3LYP/6-31G(d) level of theory as implemented in the GAMESS software suite [20]. This level of theory is a popular approach that has been commonly used for nanotube structures [21–23]. The geometric conformation of the AlNNT was obtained using the program TubeGen [24]. The length and the diameter of the optimized pure AlNNT were computed to be about 16.45 and 5.27 Å, respectively. Avoiding boundary effects, atoms at the open ends of the tube were saturated with hydrogen atoms. The adsorption energy (E_{ad}) of the N_2O molecule was defined as follows:

$$E_{ad} = E(N_2O/AlNNT) - E(AlNNT) - E(N_2O), \quad (1)$$

where $E(C_2H_2/N_2O)$ is the total energy of the adsorbed N_2O molecule on the AlNNT surface, and E(AlNNT) and $E(C_2H_2)$ are the total energies of the pristine AlNNT and the N_2O molecule, respectively. The basis set superposition error (BSSE) was corrected for in all interactions. A negative value of E_{ad} indicates exothermic adsorption.

Results and discussion

Part of the structure of the optimized AlNNT is shown in Fig. 1. It has previously been demonstrated by Tomic et al. [25] that B3LYP provides an efficient and robust basis for calculations of III–V semiconductors, capable of reliably predicting both the ground-state energies and the electronic structure. After structural optimization, the Al atoms relax inwardly while N atoms relax outwardly with respect to the tube surface. Thus, the relaxed zigzag AlNNTs can be characterized as consisting of two coaxial cylindrical tubes: an outer N cylinder and an inner Al cylinder. The optimized AlNNT has an average Al–N bond length of 1.82 Å. The difference in energy between the highest occupied molecular orbital (HOMO) and the lowest unoccupied molecular orbital (LUMO), E_g, was calculated from the DOS results. From the DOS plot of the bare AlNNT in Fig. 1, it can be concluded that this material is a semi-insulator, with a wide E_g of 4.09 eV.

N_2O adsorption on pristine AlNNT

In order to obtain stable configurations (local minima) of a single N_2O adsorbed on the tube, various possible initial adsorption geometries were verified, including single (nitrogen or oxygen), double (N–N or N–O), and triple (N–N–O) bonded atoms that are close to the Al and N atoms of the AlNNT. For simplicity, we considered the three most stable adsorption configurations (Fig. 2): the N_2O molecule is bound via one of its nitrogen atoms and its oxygen atom to the tube surface (**A**); the N_2O molecule is bound via one of its nitrogen atoms to an Al atom on the tube surface (**B**); the N_2O molecule is bound via its oxygen atom to an Al atom on the tube (**C**). More detailed information, including values of E_{ad}, E_g, and the charge transfer (Q_T) are listed in Table 1.

As shown in the table, E_{ad} ranges from −1.1 to −5.7 kcal mol^{-1}. The E_{ad} value obtained from these calculations depends on the orientation and location of the N_2O outside the AlNNT. In configuration **A**, the lengths of the newly formed Al–O and N–N bonds are about 1.93 and 1.53 Å, respectively. An isolated N_2O molecule has completely planar geometry with an N–N–O angle of 180.0 °. When the N_2O is attached to the AlNNT, significant displacement of the central N atom is

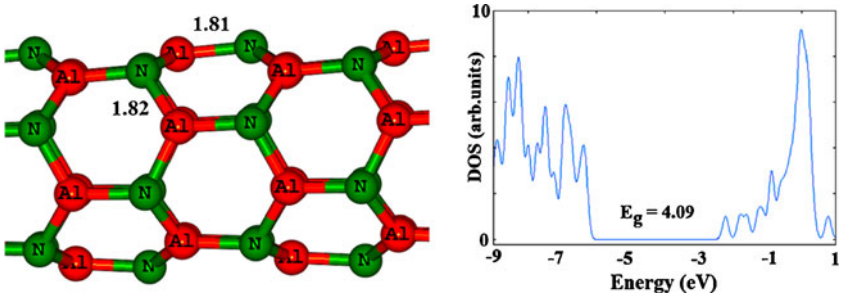

Fig. 1 Partial structural model and density of states (DOS) of the studied zigzag AlN nanotube. Distances are in Å

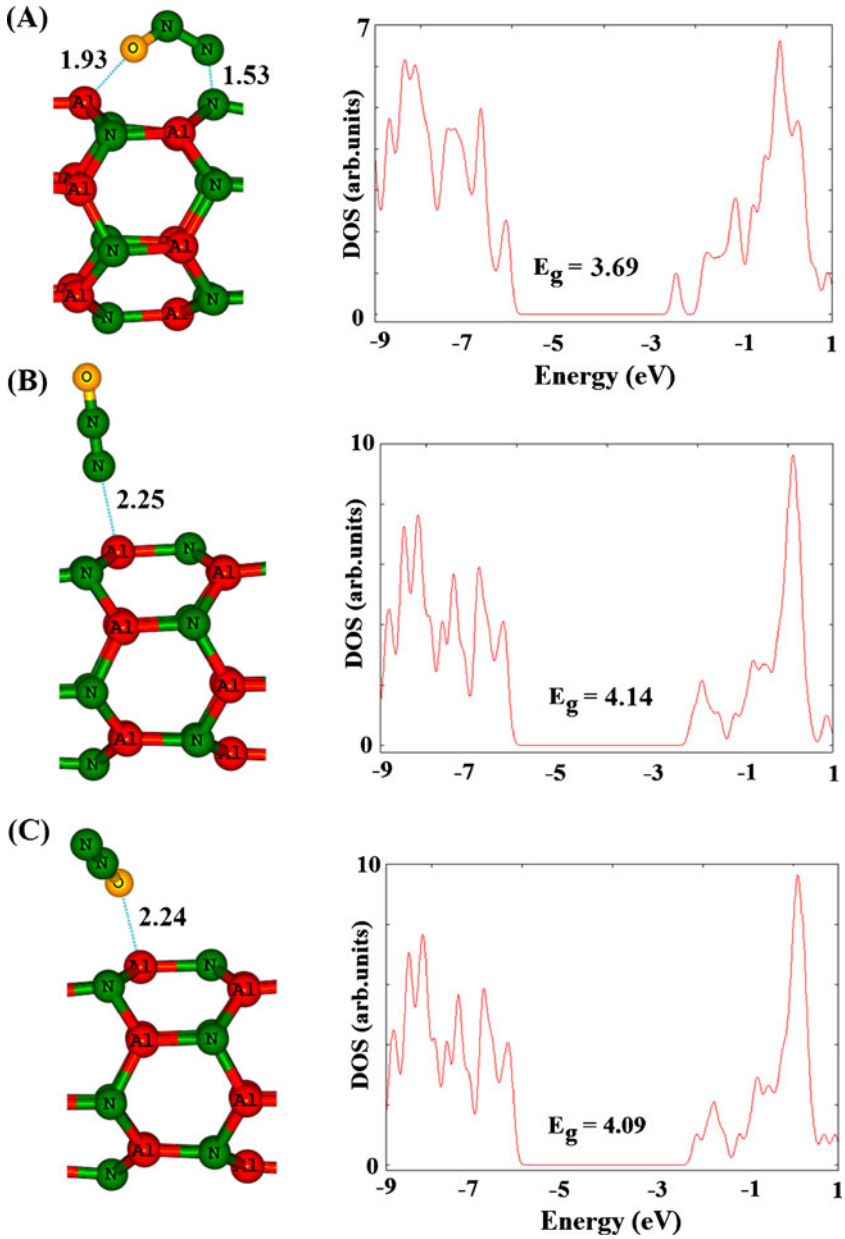

Fig. 2 Optimized structures for N_2O adsorbed onto the pristine AlN nanotube and their density of states (DOS) plots. Distances are in Å

Table 1 Calculated adsorption energies of N_2O/AlNNT complexes (E_{ad}, kcal mol^{-1}), as well as the HOMO energies (E_{HOMO}), LUMO energies (E_{LUMO}), and HOMO–LUMO energy gaps (E_g) of the systems in eV

System	E_{ad}	Q_T (e) [a]	E_{HOMO}	E_{LUMO}	E_g	ΔE_g (%)[b]
AlNNT	–	–	−6.31	−2.22	4.09	–
A[c]	−1.1	−0.430	−6.10	−2.41	3.69	9.7
B	−3.6	0.057	−6.22	−2.08	4.14	1.2
C	−5.7	0.093	−6.23	−2.14	4.09	0.0

[a] Q is defined as the average of the total Mulliken charge on the adsorbed N_2O molecule

[b] The change in the HOMO–LUMO gap of AlNNT after the adsorption of N_2O

[c] See Fig. 2

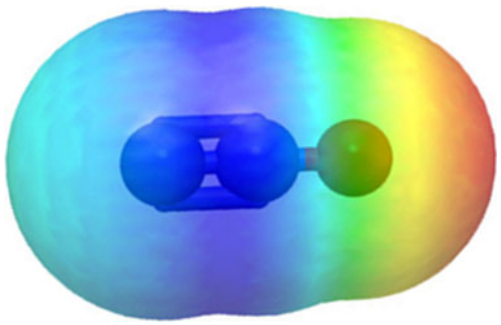

Fig. 3 Computed electrostatic potential on the molecular surface of a single N_2O molecule. Color ranges, in a.u.: *blue*, more positive than 0.010; *green*, between 0.010 and 0; *yellow*, between 0 and −0.015; *red*, more negative than −0.015

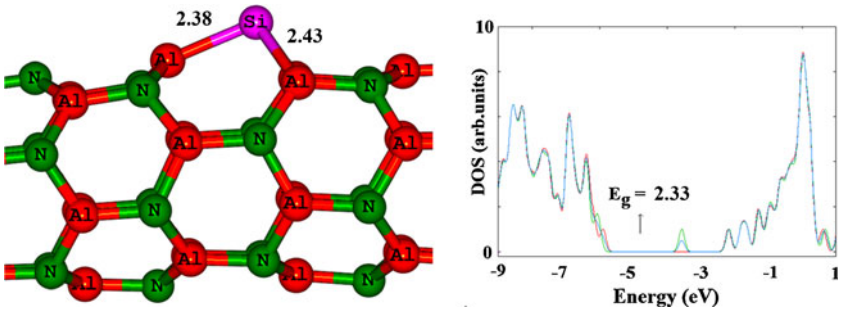

Fig. 4 Partial structural model and density of state (DOS) of the Si-doped AlNNT. Distances are in Å. Calculations were performed using the unrestricted formalism of DFT, and the beta, alpha, and total DOS spectrums are shown by *green*, *red*, and *blue* lines, respectively

predicted that reduces the N–N–O angle to 118.0 °, so the molecule is bent due to intramolecular steric repulsion. We believe that the relatively small value of E_{ad} for this configuration may be due to the large deformation of N_2O and the tube during the adsorption process.

The vibrational frequency of the N–O bond in the N_2O-adsorbed AlNNT is centered on 901 cm^{-1}. The calculated frequency for the N–O mode of the free molecule is about 2,371 cm^{-1}, indicating that the length of the N–O bond must increase during the adsorption process, and the hybridization of the central N atom of N_2O changes from *sp* to sp^2. Our calculations show that the N–O bond length increases from 1.19 to 1.32 Å after the adsorption process, which is consistent with the change in frequency. Also, NBO analysis shows that the hybridization of the central N atom changes to $sp^{1.86}$ in the complex state. As indicated in Table 1, configurations **B** and **C** are both energetically stable, with negative E_{ad} values of −3.6 and −5.7 kcal mol^{-1} and molecule–tube distances of 2.24 and 2.26 Å, respectively. The calculated molecular electrostatic surface (Fig. 3) for the N_2O shows that the relatively small E_{ad} when N_2O is adsorbed through N is due to the partial positive charge on the N atoms, which means that these atoms are not attracted to the Lewis acid sites of Al atoms in the nanotube.

To gain a deeper understanding of the effects of N_2O adsorption on the electronic properties of AlNNT, DOS plots were also constructed for the N_2O/AlNNT systems. As shown in Fig. 2, in the N_2O/AlNNT complexes, the DOS near the Fermi level and even in other places is not significantly affected by the adsorption process, and the E_g of the tube is nearly preserved (Table 1). This indicates that the interaction between the N_2O molecule and the pristine AlNNT is very weak and the process is *electronically harmless*. This may be interesting from a gas-sensing standpoint. It was recently revealed that the pristine zigzag AlNNT is not sensitive to NH_3 [26], CO [27], N_2 [28], CO_2 [28], H_2S [29], and H_2O [30] molecules, while it may be used to detect formaldehyde [30], SO_2 [31], O_2 [32], and NO_2 [33]. Moreover, it can be concluded that gas detection may be feasible in the presence of N_2O gaseous molecules.

N_2O adsorption on Si-doped AlNNT

Furthermore, the effects of replacing an N atom in the tube wall (which effectively does not participate in the interaction) with a Si atom on the geometric and electronic properties of the AlNNT as well as on the adsorption behavior were investigated. Upon replacing an N atom with an Si impurity, the geometric structure of the AlNNT is dramatically distorted (Fig. 4). The Si atom is projected out of the tube surface in order to reduce stress due to its larger size than the N atom in the optimized Si-doped tube. The calculated bond lengths are 2.38 and 2.43 Å for the Si–Al bonds in the Si-doped AlNNT, much longer than the corresponding Al–N bonds in the pristine tube. Also, the Al–Si–Al angles in the Si-doped tube are 86.9 ° and 98.8 °, which are smaller than Al–N–Al angles in the pristine tube (109.9 ° and 116.1 °). This geometric distortion results in a marked change in the electronic properties of the AlNNT. As shown by the calculated DOSs and the E_g in Fig. 4 and Table 2, for the electron-deficient Si-doped AlNNT system, the E_g value decreases to 2.33 eV, and a new local energy level appears at the top of the valence level at −3.56 eV,

Table 2 Calculated adsorption energies of N_2O/Si-doped AlNNT complexes (E_{ad}, kcal mol^{-1}), as well as the SOMO energies (E_{SOMO}), LUMO energies (E_{LUMO}), and HOMO–LUMO energy gaps (E_g) of the systems in eV

System	E_{ad}	Q_T (e) [a]	E_{SOMO}	E_{LUMO}	E_g	ΔE_g (%) [b]
Si-doped AlNNT	–	–	−5.89	−3.56	2.33	–
P[c]	−4.8	0.082	−5.68	−3.36	2.32	0.4
Q	−25.3	−0.574	−5.78	−3.68	2.10	9.4
R	−103.6	–	−5.15	−2.83	2.32	0.4

[a] *Q* is defined as the average of the total Mulliken charge on the adsorbed N_2O molecule

[b] The change in the SOMO–LUMO gap of AlNNT after the adsorption of N_2O

[c] See Fig. 5

which may act as a capture center for atoms or molecules that cannot be trapped by the pristine AlNNT. In this situation, the doping of the Si atom results in an electronic hole, thereby increasing the conductivity of the AlNNT. This fact suggests that the Si-doped AlNNT is a typical p-type semiconductor. From the above results, it is understandable that the Si impurity introduces local states inside the E_g, which may improve the reactivity of AlNNT. It should be noted that we also use E_g to symbolize the SOMO (singly occupied molecular orbital)/LUMO energy gap for open-shell systems here.

Subsequently, we explored N_2O adsorption on the Si-doped tube by placing the molecule in different initial orientations above the Si atom: with with either the O or an N atom of the molecule close to Si. After careful relaxation to optimize the initial structures, three different final minima structures were obtained, which are shown in Fig. 5. The interactions can be categorized into three types: (i) physisorption (configuration **P**), (ii) chemisorption (configuration **Q**), and (iii) dissociation of N_2O (configuration **R**). In Table 2 we have summarized

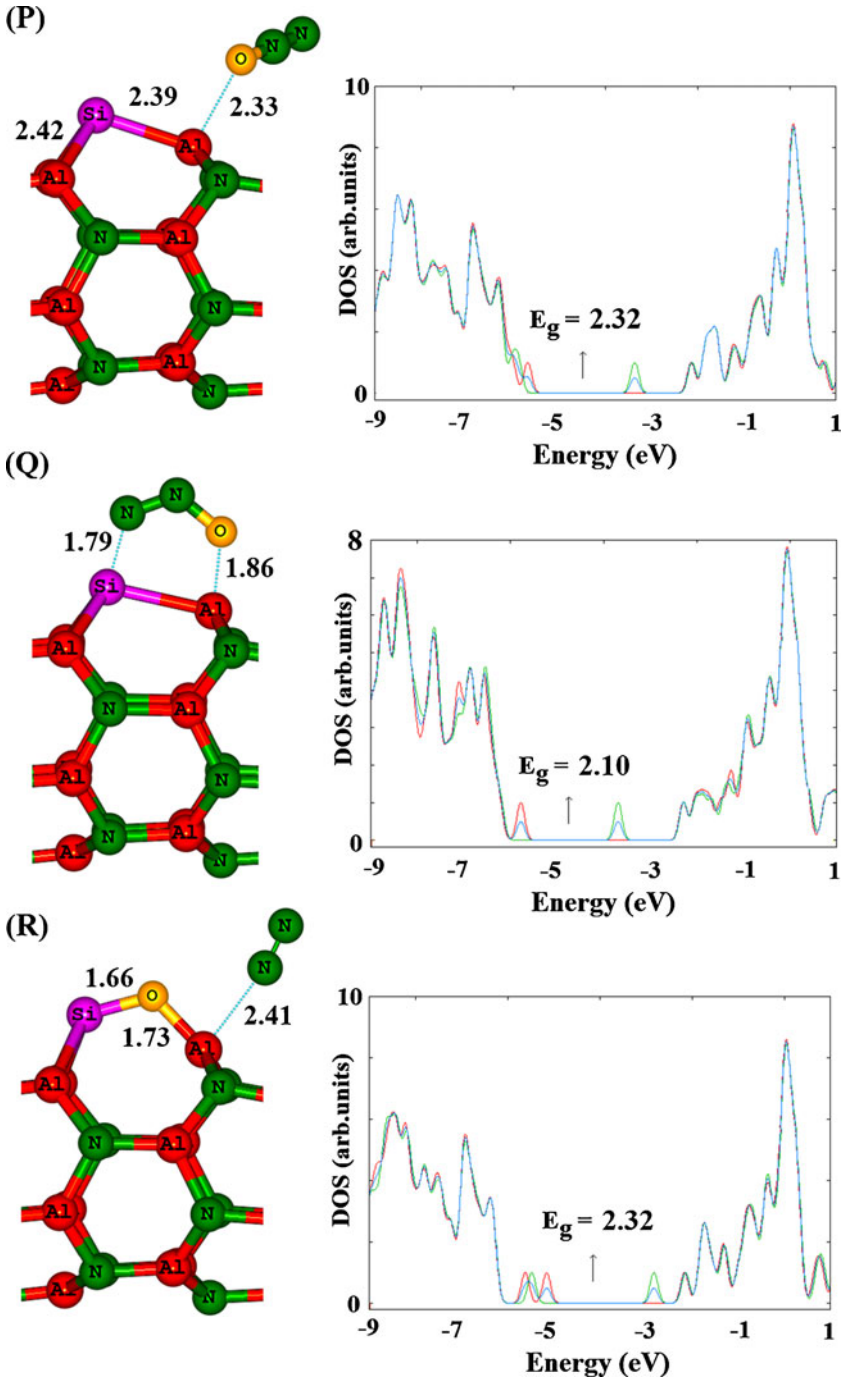

Fig. 5 Optimized structures for N_2O adsorbed onto the Si-doped AlNNT and their density of states (DOS) plots. Distances are in Å. Calculations were performed using the unrestricted formalism of DFT, and the beta, alpha, and total DOS spectrums are shown by *green*, *red*, and *blue* lines, respectively

the results for E_{ad}, charge transfer, and E_g for N_2O adsorption onto Si-doped AlNNT.

In the physisorption case (**P**), during the optimization, the N_2O reoriented in such a way that its O atom got close to the Al site (the nearest Al atom to the Si impurity), with an E_{ad} of −4.8 kcal mol^{-1}. Also, the corresponding interaction distance between the Al atom of AlNNT and the O atom of N_2O was about 2.33 Å. This small E_{ad} value and large interaction distance indicate that the N_2O molecule undergoes weak physical adsorption onto the AlNNT due to van der Waals forces.

As shown in Fig. 5, in configuration **Q**, the distances between the N and O atoms of N_2O and the Si and Al atoms of the tube are about 1.79 and 1.86 Å, respectively. The E_{ad} value for this configuration is about −25.3 kcal mol^{-1}, with a charge transfer of about 0.574 *e* from the tube to the N_2O (Table 2). Furthermore, the adsorption of the molecule induces slight structural deformations of both the adsorbed molecule and the AlNNT (Fig. 5Q). The angles Al–Si–Al and N–Al–N of the nanotube change to 92.9 ° and 105.1 ° in the adsorbed form, and the N_2O-adsorbed Al–Si bond is pulled outward from the tube surface, increasing the bond length from 2.38 to 2.54 Å. These results indicate that the adsorption process may be chemical.

The most interesting case, however, is the dissociation of the N_2O molecule on the Si-doped AlNNT through configuration **R**. In this case, the N–O bond of the molecule is initially vertically above and close to the Si atom, and then a full relaxation to achieve optimization was performed (Fig. 5R). Based on the NBO results and geometry analysis, the Si–Al bond of the tube is broken after the adsorption process, the oxygen atom of the molecule diffuses into the tube surface, and two new bonds are formed: Si–O and O–Al, with corresponding lengths of 1.66 and 1.73 Å, respectively. Interestingly, in this configuration, an N_2 molecule escapes from the wall of the tube, leaving an O atom attached to the Si atom of AlNNT. This configuration is the most stable of all the obtained adsorption configurations, with an E_{ad} of −103.6 kcal mol^{-1}. This suggests that N_2O molecules could be reduced to N_2 molecules on Si-doped tubes. To determine the influence of N_2O adsorption on the electronic properties of the tube, we constructed the DOS plots of the complexes, as shown in Fig. 5. The E_g values of all the configurations ranged between 2.32 and 2.10 eV, indicating that the E_g of the tube is not significantly changed by the adsorption process (it is 2.32, 2.32, and 2.10 eV for the **P**, **R**, and **Q** configurations, respectively).

We also calculated the energy barriers for probable transformations of the **P** and **Q** configurations to the **R** one using the synchronous transit-guided quasi-Newton (STQN) method [34]. It was found that the **P** configuration has to overcome an energy barrier of 20.4 kcal mol^{-1} to transform to the configuration **R**. Also, the configuration **Q** needs to overcome an energy barrier of 23.7 kcal mol^{-1} to convert to a configuration similar to the **R** one in which the N_2 molecule released is located on the Si atom. These energy barriers appear to be small enough for these transformations to be likely to occur at room temperature.

Conclusions

The geometric structures and electronic properties of pristine and Si-doped AlNNTs in the presence and absence of an N_2O molecule were explored using density functional theory. It was found that the N_2O molecule interacts with the pristine AlNNT via van der Waals forces, but it presents much higher reactivity toward the Si-doped AlNNT such that the oxygen atom of the molecule is diffused into the tube wall. The adsorption energies corresponding to the adsorption of N_2O on the pristine and Si-doped AlNNTs were calculated to be in the range +7.1 to −5.7 kcal mol^{-1} and −4.8 to −103.6 kcal mol^{-1}, respectively. The results indicated that the N_2O molecule could be reduced to N_2 on the Si-doped tube.

References

1. Centi G, Galli A, Montanari B, Perathoner S, Vaccari A (1997) Catal Today 35:113–124
2. Centi G, Dall'Olio L, Perathoner S (2000) J Catal 192:224–235
3. Burch R, Daniells ST, Breen JP, Hu P (2004) J Catal 224:252–260
4. Chen Y, Gao B, Zhao JX, Cai QH, Fu HG (2012) J Mol Model 18:2043–2054
5. Iijima S (1991) Nature 354:56–58
6. Politzer P, Lane P, Murray JS, Concha MC (2005) J Mol Model 11:1–7
7. Dinadayalane TC, Kaczmarek A, Lukaszewicz J, Leszczynski J (2007) J Phys Chem C 111:7376–7383
8. Dinadayalene TC, Murray JS, Concha MC, Politzer P, Leszczynski J (2010) J Chem Theory Comput 6:1351–1357
9. Peralta-Inga Z, Boyd S, Murray JS, O'Connor CJ, Politzer P (2003) Struct Chem 14:431–443
10. Rubio A, Corkill JL, Cohen ML (1994) Phys Rev B 49:5081–5084
11. Cumings J, Zettl A (2000) Chem Phys Lett 316:211–216
12. Zhang D, Zhang R (2003) Chem Phys Lett 371:426–432
13. Tondare V, Balasubramanian C, Shende S, Joag D, Godbole V, Bhoraskar S, Bhadhade M (2002) Appl Phys Lett 80:4813–4815
14. Balasubramanian C, Bellucci S, Castrucci P, Crescenzi M, Bhoraskar S (2004) Chem Phys Lett 383:188–191
15. Yin B, Bando Y, Zhu Y, Li M, Tang C, Golberg D (2005) Adv Mater 17:213–217
16. Fan Y (2011) Mater Lett 65:1900–1902
17. Tabtimsai C, Keawwangchai S, Nunthaboot N, Ruangpornvisuti V, Wanno B (2012) J Mol Model 18:3941–3949
18. Yim WL, Liu ZF (2004) Chem Phys Lett 398:297–303
19. Grujicic M, Cao G, Gersten B (2003) Appl Surf Sci 206:167–177
20. Schmidt M et al (1993) J Comput Chem 14:1347–1363
21. Ahmadi A, Beheshtian J, Kamfiroozi M (2012) J Mol Model 18:1729–1734
22. Moradi M, Peyghan A, Bagheri Z, Kamfiroozi M (2012) J Mol Model 18:3535–3540

23. Beheshtian J, Bagheri Z, Kamfiroozi M, Ahmadi A (2012) J Mol Model 18:2653–2658
24. Frey JT, Doren DJ (2005) TubeGen software, version 3.3. http://turin.nss.udel.edu/research/tubegenonline.html
25. Tomić S, Montanari B, Harrison NM (2008) Phys E 40:2125–2127
26. Ahmadi A, Beheshtian J, Hadipour NL (2011) Phys E 43:1717–1719
27. Beheshtian J, Bagheri Z, Kamfiroozi M, Ahmadi A (2012) Struct Chem 23:653–657
28. Jiao Y, Du A, Zhu Z, Rudolph V, Smith SC (2010) J Mater Chem 20:10426–10430
29. Beheshtian J, Peyghan AA, Bagheri Z (2012) Phys E 44:1963–1968
30. Ahmadi A, Hadipour NL, Kamfiroozi M, Bagheri Z (2012) Sens Actuators B Chem 161:1025–1029
31. Beheshtian J, Baei MT, Peyghan AA, Bagheri Z (2012) J Mol Model 18:4745–4750
32. Baei MT, Peyghan AA, Bagheri Z (2012) Chin Chem Lett 23:965–968
33. Beheshtian J, Baei MT, Bagheri Z, Peyghan AA (2012) Microelectron J 43:452–455
34. Peng C, Schlegel HB (1993) Israel J Chem 33:449–454